A Trade-off between Local and Distributed Information Processing Associated with Remote Episodic versus Semantic Memory

Jennifer J. Heisz[1,2], Vasily Vakorin[2], Bernhard Ross[2], Brian Levine[2*], and Anthony R. McIntosh[2*]

Abstract

■ Episodic memory and semantic memory produce very different subjective experiences yet rely on overlapping networks of brain regions for processing. Traditional approaches for characterizing functional brain networks emphasize static states of function and thus are blind to the dynamic information processing within and across brain regions. This study used information theoretic measures of entropy to quantify changes in the complexity of the brain's response as measured by magnetoencephalography while participants listened to audio recordings describing past personal episodic and general semantic events. Personal episodic recordings evoked richer subjective mnemonic experiences and more complex brain responses than general semantic recordings. Critically, we observed a trade-off between the relative contribution of local versus distributed entropy, such that personal episodic recordings produced relatively more local entropy whereas general semantic recordings produced relatively more distributed entropy. Changes in the relative contributions of local and distributed entropy to the total complexity of the system provides a potential mechanism that allows the same network of brain regions to represent cognitive information as either specific episodes or more general semantic knowledge. ■

INTRODUCTION

Accumulating evidence points to the counterintuitive notion that "noisier" or more complex brain signals are associated with greater capacity for meaningful cognitive information processing than more predictable responses (Heisz, Shedden, & McIntosh, 2012; Misic, Mills, Taylor, & McIntosh, 2010). Brain signal complexity refers to the irregularity of the amplitude pattern of an EEG or magnetoencephalography (MEG) recording over time (Mišić, Vakorin, Paus, & McIntosh, 2011; Vakorin, Mišić, Krakovska, & McIntosh, 2011). Previous work has shown that brain signal complexity increases with learning (Heisz et al., 2012) and with the amount of cognitive information available for a particular stimulus (Heisz et al., 2012; Misic et al., 2010). The complexity of the brain's response is also correlated with more accurate and stable cognitive performance (McIntosh, Kovacevic, & Itier, 2008). Furthermore, changes in brain signal complexity follow a typical developmental trajectory such that both cognitive ability and brain signal complexity progressively increase from infancy to adulthood (Lippe, Kovacevic, & McIntosh, 2009; McIntosh et al., 2008). With advancing age, brain signal complexity decreases with the severity of cognitive impairment and is lowest for individuals with dementia (Park, Kim, Kim, Cichocki, & Kim, 2007). The working hypothesis is that brain signal complexity reflects the information processing capacity of the underlying functional network and provides an index of the repertoire of potential responses that can be produced (Deco, Jirsa, & McIntosh, 2011); irregularity in the amplitude pattern over time is the manifestation of the network exploring its many potential configurations.

Neural network dynamics can be understood in terms of ensembles of coupled neural systems interacting in a nonlinear way. Such interactions produce a response that is remarkably irregular yet nonrandom (Jirsa & McIntosh, 2007; Nunez & Srinivasan, 2005). These dynamic interactions among network components are believed to bind information across widespread regions of the brain (Engel, Fries, & Singer, 2001; Varela, Lachaux, Rodriguez, & Martinerie, 2001). Specifically, information is integrated across widespread networks through the emergence and disappearance of correlated activity between network nodes across multiple timescales, as revealed through computer simulations (Sakurai, 1999; Tononi, Edelman, & Sporns, 1998). These transient changes in the global connectivity pattern produce realistic fluctuations in resting state brain signals (Deco, Jirsa, McIntosh, Sporns, & Kötter, 2009; Ghosh, Rho, McIntosh, Kotter, & Jirsa, 2008). It follows that the complexity we observe in empirically recorded brain signals (e.g., EEG, MEG) captures the functional response of the underlying neural network. In

[1]McMaster University, Hamilton, Canada, [2]Baycrest Health Sciences, Toronto, Canada
*These authors share senior authorship.

Journal of Cognitive Neuroscience 26:1, pp. 41–53
doi:10.1162/jocn_a_00466

other words, brain signal complexity provides a window onto the underlying dynamic system (Stam, 2005) and may help us to understand how cognition emerges from such activity (Bressler & Mcintosh, 2007). Critically, this index of network complexity cannot be obtained by simply counting the number of active brain regions and plotting a graph; although the characterization of network architecture is important, it represents the static picture that is blind to the transient and dynamic interactions between network nodes. To understand how cognition emerges from brain function, one must examine the functional dynamics of neural networks across multiple timescales (Honey, Kotter, Breakspear, & Sporns, 2007; Sporns, Chialvo, Kaiser, & Hilgetag, 2004; Breakspear, 2002; Freeman & Rogers, 2002; Friston, 2000).

Brain signal complexity of EEG and MEG recordings can be estimated using measures of entropy. Entropy is an information theory tool that indexes the irregularity of a signal, such that irregular signals have higher entropy than more predictable ones (Gatlin, 1972; Shannon, 1948). An advantage of using information theoretic tools to quantify the complexity of brain signals is the association between signal entropy and information content (Shannon, 1948): More irregular signals have the potential to transmit more information. Thus, information theoretic measures may help to reveal how meaningful cognitive information is represented and communicated within the brain.

This study applied information theoretic tools to examine the relation between neuromagnetic brain signal complexity and information processing during a complex memory task. As in previous studies, we used multiscale entropy (MSE) to estimate the total information processing capacity of each brain region across multiple timescales (Heisz & McIntosh, 2013; Costa, Goldberger, & Peng, 2005). We further parsed the total entropy of a signal into its two component parts: (1) distributed entropy, which is the estimate of the information that each brain region shares with the rest of the network and provides a nonlinear estimate of connectivity (Vakorin, Lippé, & McIntosh, 2011), and (2) local entropy, which is an estimate of the amount of information processed by each brain region independently from the rest of the network (Vakorin, Mišić, et al., 2011).

We manipulated the richness of cognitive information by exposing participants to cues that evoke a richly detailed autobiographical memory or factual (semantic) information. According to classic models, memory is represented in a distributed network whereby unique but related aspects of the memory are stored in different functional configurations of the network (McClelland & Rumelhart, 1985). Transient changes in the functional configuration of the network over time would be reflected in the complexity of the brain signal across multiple timescales such that a network with more potential configurations has a higher information processing capacity and the potential to produce a more irregular response (Stam, 2005). Autobiographical memory serves as an excellent model for assessing this hypothesis because it engages dynamic and widely distributed systems involved in memory, emotion, and perceptual imagery.

Participants were presented with self-recorded audio sequences documenting either autobiographical episodes from the past year or semantic information unrelated to autobiographical memory (Levine et al., 2004). We measured the participants' neuromagnetic activity with MEG while they listened to the recordings. This unique approach of self-recorded documentation allowed us to create a rich data set of remote memories from which we selected a subset of age-matched events to reduce the predictability of test items. Episodic autobiographical information is mediated by a left-lateralized brain network that includes midline and ventrolateral frontal regions, the medial-temporal lobe, the TPJ, and retrosplenial/posterior cingulate regions (Cabeza & St Jacques, 2007; Svoboda, McKinnon, & Levine, 2006; Maguire, 2001); these regions only partially overlap with those engaged by laboratory measures of episodic memory, such as word lists (McDermott, Szpunar, & Christ, 2009; Gilboa, 2004). Autobiographical memory is grounded in semantic knowledge (general knowledge about the world and oneself; Renoult, Davidson, Palombo, Moscovitch, & Levine, 2012) and engages similar distributed neural networks for processing (Burianova, McIntosh, & Grady, 2010; Burianova & Grady, 2007; Rajah & McIntosh, 2005; Levine et al., 2004).

Although the activation patterns associated with autobiographical memory and semantic knowledge have been investigated in depth, their neural correlates have not been studied with information theoretic measures sensitive to complexity. We expected personal episodic (PE) recordings to produce greater brain signal complexity than general semantic (GS) recordings because of the richer detail that is associated with PEs. However, it was unclear whether the different mnemonic experiences would elicit a relative change in the contribution of local versus distributed entropy to the total complexity of the system. It was possible that the greater details associated with PE recordings would increase both local and distributed entropy. Alternatively, given that local and distributed entropy reflect different aspects of network information processing, it was also possible that the relative contribution of local versus distributed entropy may differ across condition. Given that distributed entropy captures the shared information between brain regions, a relative increase in distributed processing may be one way to represent information that is shared among associated events and thus would be greater for the GS recordings. In contrast, a relative increase in local processing may accompany PE memory as a way of representing the specific details associated with an event. Considering the novelty of applying information theoretic tools to understand information processing during a memory task, we did not constrain our analysis to autobiographical and semantic networks derived from mean-based approaches. Instead, we used a data-driven multivariate approach partial least squares (PLS) to statistically analyze the condition

differences in complexity over multiple timescales across the entire set of brain regions (Lobaugh, West, & McIntosh, 2001).

To further characterize the dynamics of the signal, we used spectral power to quantify the frequency composition of the waveforms. Entropy and spectral power are related in that both measures are sensitive to the frequency composition of the waveform; however, entropy captures both task-related phase/nonlinear changes, in addition to power changes, and thus may be less sensitive to the task effects. We also statistically analyzed these data using PLS (Lobaugh et al., 2001) for ease of comparison with the complexity measures.

METHODS

Participants

Participants were eight healthy adults (mean age = 29.6 ± 4.72 years, range = 25–40, four women). Informed consent was obtained from each participant in written form, and the Research Ethics Board of Baycrest approved all procedures.

Stimuli

Participants prospectively collected audio sequences over 2–7 months using a portable digital recorder (ICD-BP100 V-O-R; Sony, San Diego, CA) following the methods specified by Svoboda and Levine (2009) and Levine et al. (2004). Extensive training on the recording method was provided along with a detailed instruction manual and feedback on several practice recordings. A cue card was attached to each recorder for guidance.

There were two recording conditions, PE memory and GS memory. PE recordings were 1- to 2-min descriptions of a unique autobiographical episode, defined according to theoretical works on this topic (Tulving, 2002; Wheeler, Stuss, & Tulving, 1997), including the story line, location, perceptions, thoughts, and emotional reactions. Very significant emotional events were excluded. Participants were instructed to make PE recordings during or soon after the event occurred and within the same day (mean time elapsed since the event = 186 min, *SD* = 117 min). GS recordings were 1- to 2-min readings from a book about neighborhoods in Toronto, Canada (excluding those evoking a specific autobiographical event) and were yoked in time to the PE recordings (for PE: *M* = 199 days, range = 22–440 days; for GS: *M* = 163 days, range = 42–195 days; $t(1, 7) = 0.64$, *ns*). Participants included a title in each recording (e.g., "Michael and Erika's wedding," "Bloor West Village"). Following PE recordings, participants indicated time elapsed since the event and provided ratings on a 4-point scale for the event uniqueness (1 = *routine*, 4 = *completely novel*), personal importance (1 = *not important*, 4 = *highly important*), and emotional change as a result of the event (1 = *no change*, 4 = *major change*). The average of these three ratings across the eight participants was 2.35 (*SD* = 0.46), indicating a moderate level of overall novelty and significance. This confirmed that participants followed the instruction to recorded daily events that were unique, although not of great personal significance. Participants were instructed not to listen to their recordings after dictating them.

The median number of recordings made by each participant for the PE and GS conditions were 71 and 41, respectively (for PE, range = 58–500; for GS, range = 16–206). Twelve recordings per condition per participant were randomly selected for use in the study. The large number of recordings made by each participant reduced the novelty of the recording activity as well as the predictability of which recordings would be used in the study. Although the act of recording may have changed the neural representation of the memory, behavioral research has shown that this has little effect on recall (Thompson, 1982). Accordingly, the participants did not report recollection of the habitual recording act itself, although the information in the recording was very effective in evoking recollection of the PEs (see analysis of ratings below).

Task Procedures

The experiment consisted of 24 trials of 90 sec in duration. Each trial began with a 30-sec rest period during which the participant maintained fixation on a central cross. Two seconds before the end of the rest period, the participant heard the title that they had created and closed their eyes. While listening to the recording, they were instructed to mentally reexperience the events (PE) or to think about the semantic information (GS). PE and GS recordings were randomized, in equal number, across the trials. Immediately after listening to the recording, the participant rated the vividness of the memory according to the reexperiencing of thoughts and emotions, visual imagery, how easily the memory came to mind (episodic fluency), and overall reexperiencing. Ratings were made on four 10-point scales, with 10 being most vivid. Ratings were collected for both PE and GS recordings to assess for the presence of intrusive episodic thoughts in GS and to confirm that PE recordings evoked a higher degree of reexperiencing.

MEG: Recording and Preprocessing

Neuromagnetic recordings were made using a 151-channel axial gradiometer type MEG system based on SQUID technology (CTF, VSM MedTech Ltd., Port Coquitlam, BC, Canada) in a magnetically shielded room. The MEG signals were sampled at a rate of 312.5 Hz after 100-Hz low-pass filtering, digitized, and continuously stored. Head localization coils were placed on the nasion and left and right preauricular points for coregistration of the MEG sensor with a standard anatomical MR image (Montreal Neurological Institute template).

Off-line, the data were low-pass filtered at 40 Hz. Eye blinks were detected based on a spatiotemporal model. A PCA was applied to the averaged eye-blink time series, and the spatial pattern of the largest principal component was removed from the data. Source activity was reconstructed with synthetic aperture magnetometry (Robinson & Vrba, 1999), which is based on a linearly constrained minimum variance beamformer (Van Veen, Van Drongelen, Yuchtman, & Suzuki, 1997). Individual head models for this procedure were constructed by locally approximating spheres for each MEG sensor to the digitized head shape. The participant's head shape was obtained with a 3-D digitization device (Polhemus Fastrak, Polhemus, Colchester, VT). The source images were coregistered with a standard anatomical MR (colin27; Holmes et al., 1998) based on fiducial locations at the nasion and the left and right preauricular points; this procedure of using individual head models and group analysis based on a standard brain has been validated (Steinstraeter et al., 2009). A set of weighting coefficients was determined for 72 ROIs (Bezgin, Vakorin, van Opstal, McIntosh, & Bakker, 2012; Kotter & Wanke, 2005). The linear combination of the weighting coefficients with the MEG data resulted in virtual sensor waveforms of the source activity at each ROI.

Data were parsed into 30-sec epochs of episodic and semantic retrieval. We discarded the last 6-sec interval of each trial to control for any variance associated with the offset of the audio recording. To capture potential changes in the brain's response over the trial while maintaining a sufficient number of data point per bin (e.g., 1875 data points) for the entropy analysis, we evenly divided the 24-sec epochs into four 6-sec bins.

Information Theoretic Analyses

Down-sampling

To capture the dynamic changes in the network activity at different timescales, we created multiple coarse-grained time series from the original MEG time series by progressively down-sampling the MEG poststimulus time series $\{x_1,\ldots, x_i,\ldots, x_N\}$ per trial and per condition (Figure 1B). For timescale τ, the coarse-grained time series $\{y^{(\tau)}\}$ is constructed by averaging data points within nonoverlapping windows of length τ. Each element of a coarse-grained time series, j, is calculated according to Equation 1:

$$y_j^{(\tau)} = \frac{1}{\tau} \sum_{i=(j-1)\tau+1}^{j\tau} x_i,\ 1 \le j \le \frac{N}{\tau}. \qquad (1)$$

Down-sampling is similar to low-pass filtering; for a particular timescale, dividing the sampling frequency by that timescale approximates the frequency at which the signal is low-pass filtered. We used this down-sampling procedure to create Timescales 1–20 and analyzed each coarse-grained time series using the three information theoretic measures: MSE, distributed entropy, and local entropy, described below. Timescales 1–20 were converted into milliseconds by dividing the timescale by the sampling rate (312.5 Hz).

MSE

We used MSE to estimate the total information processing capacity of each brain regions (Heisz & McIntosh, 2013; Costa et al., 2005). To calculate MSE, we used the algorithm available at www.physionet.org/physiotools/mse. The algorithm calculates the sample entropy for each coarse-grained time series (Equation 2):

$$S_E(m, r, N) = \ln \frac{\sum_{i=1}^{N-m} n_i' m}{\sum_{i=1}^{N-m} n_i' m + 1}, \qquad (2)$$

where m is the pattern length, r is the similarity criterion, and $n'_i{}^m$ is the number of matches. Sample entropy quantifies the complex of a time series by estimating the predictability of amplitude patterns across a time series of length N (Figure 1A). The pattern length (i.e., embedding dimension) m was set to 2, which means that the complexity of the amplitude pattern of each time series was calculated by considering a sequence pattern for two versus three consecutive data points, respectively. The pattern length was held constant across the time series for all the subjects and trials. To achieve sufficient number of data points for the coarsest grained time series, we set the pattern length to 2 to increase the robustness of the results. The similarity criterion r was set to 0.5; this means that data points were considered to have indistinguishable amplitude values (i.e., to "match") if the absolute amplitude difference between them was ≤50% of the time series standard deviation. The parameter values for m and r were set following the guidelines outlined by Richman and Moorman (2000) for time series with more than 100 data points (for a detailed procedure on selecting parameters, refer to Lake, Richman, Griffin, & Moorman, 2002). For each subject, a source-specific MSE estimate was obtained as a mean across single trial entropy measures for Timescales 1–20.

Distributed Entropy

Distributed entropy, which is akin to mutual information, was used to estimate the amount of information shared between two brain sources (Kraskov, Stögbauer, & Grassberger, 2004). Similar to estimations of the linear cross-correlation (e.g., phase-locking), distributed entropy is sensitive to the affiliation between the two sources; however, unlike linear cross correlation, distributed entropy (estimated under the framework of nonlinear dynamics) is additionally sensitive to nonlinear dependencies and thus may be more sensitive to subtle differences in task. By construction, distributed entropy is nonnegative: Zero distributed entropy means that the dynamics of the two sources are strictly

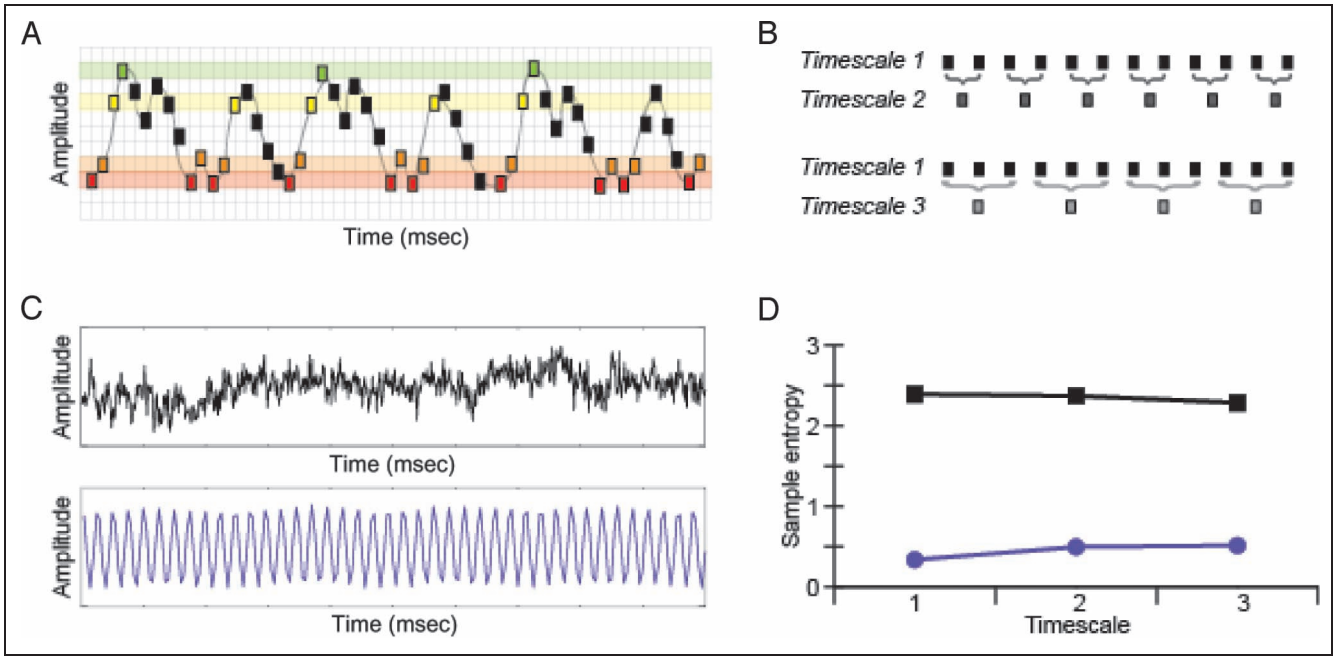

Figure 1. (A) Sample entropy estimates the variability of a time series. The pattern length m was set to 2, which means that the variance of the amplitude pattern of each time series will be represented in two-dimensional versus three-dimensional space by considering the sequence pattern of two versus three consecutive data points, respectively. The similarity criterion r reflects the amplitude range (denoted by the height of the colored bands) within which data points are considered to "match." To calculate sample entropy for this simulated time series, begin with the first two-component sequence pattern, red-orange. First, count the number of times the red-orange sequence pattern occurs in the time series; there are 10 matches for this two-component sequence. Second, count the number of times first three-component sequence pattern, red-orange-yellow, occurs in the time series; there are five matches for this three-component sequence. Continue in this manner for the next two-component sequence (orange-yellow) and three-component sequence (orange-yellow-green). The number of two-component matches (5) and three-component matches (3) for these sequences are added to the previous values (total two-component matches = 15; total three-component matches = 8). Repeat for all other sequence matches in the time series (up to $N - m$) to determine the total ratio of two-component matches to three-component matches. Sample entropy is the natural logarithm of this ratio. (B) Down-sampling generates multiple time series of varying timescales. Timescale 1 is the original time series. To create the time series of subsequent timescales, simply divide the original time series into nonoverlapping windows of the timescale length and average the data points within each window. Sample entropy is calculated for each timescale, hence MSE. Sample entropy and down-sampling illustrations were adopted from Costa et al. (2005). (C) Two simulated waveforms: a regular or predictable waveform depicted in purple and a more stochastic waveform depicted in black. (D) Sample entropy values of the two simulated waveforms for the first three timescales. Sample entropy values are near zero for the regular waveform and around 2.5 for the more variable waveform. An increase in sample entropy corresponds to an increase in signal complexity, which, according to information theory, can be interpreted as an increase in the amount of information processing capacity of the underlying system.

independent, and distributed entropy values greater than zero indicate the degree of affiliation.

To calculate distributed entropy, we first estimated total and joint entropies using Shannon entropy (Shannon, 1948) through the corresponding correlation integrals as proposed by Prichard and Theiler (Vakorin, Lippé, et al., 2011; Prichard & Theiler, 1995).

Total entropy represents the variability associated with the dynamics of a single source, $H(X)$ (Shannon, 1948). We computed total entropy for $m = 2$ by estimating the variance of the amplitude pattern of each time series by considering the sequence patterns of two consecutive data points only, rather than the ratio of two versus three consecutive points done for sample entropy. However, the results were similar for both sample entropy and total entropy.

Joint entropy represents the combined variability associated with the dynamics of two sources, $H(X,Y)$. We computed joint entropy for $m = 2$ by estimating the variance of the sequence pattern of two consecutive data points for two different sources simultaneously. To alleviate the potential noise effects in the calculation of joint entropy, we increased the tolerance threshold to $r = 1$. As expected, this slight adjustment to parameter r did not affect the relative differences in entropy values between conditions (Richman & Moorman, 2000).

Distributed entropy was computed by subtracting the joint entropy from the sum of the total entropy of each source: $I(X;Y) = H(X) + H(Y) - H(X,Y)$ using in-house software developed using Matlab and C scripts. To obtain entropy estimates for X with respect to the entire system (i.e., all sources), conditional entropy $H(X|Y)$ and distributed entropy $I(X;Y)$ were averaged over all sources Y (Vakorin, Mišić, et al., 2011).

Local Entropy

Local entropy provided an estimate of the amount of information processed by each brain region independently

from the other brain regions in the network (Vakorin, Lippé, et al., 2011). In other words, local entropy represents the portion of total information that was processed locally and thus not shared with other sources. We estimated local entropy by subtracting distributed entropy from total entropy: $H(X|Y) = H(X) - I(X;Y)$ using in-house software developed using Matlab and C scripts.

Spectral Power Analysis

As a complement to the entropy analyses, we computed spectral power for the same data set to characterize the spectral composition of the waveforms. Spectral power density of each discrete time series x (i.e., for each subject, condition, channel, and trial) was estimated by Welch's averaged, modified periodogram method of spectral power estimation using the built-in Matlab function for cross-power spectral density in which Pxx = cpsd (x, x, [ ], [ ], [ ], fs), where fs denotes the sampling frequency (Welch, 1967).

Statistical Assessment by PLS

To determine the effect of our experimental manipulation on each MEG statistic (MSE, distributed entropy, local entropy, spectral power), we conducted a whole-brain analysis using PLS. PLS is a multivariate technique designed to identify latent factors that account for most of the variance in the data (Lobaugh et al., 2001). To prepare the data for PLS analysis, the data matrices were organized in the form of [Subjects × Condition] in rows and [Sources × Timescale/Frequency] in columns. For the present analyses, we took the mean-centered approach wherein the mean-centered data matrix (computed by subtracting each individual data point from the grand mean across conditions) was decomposed into a set of mutually orthogonal factors.

Singular value decomposition was used to project the mean-centered data matrix onto a set of orthogonal latent variables (LVs), with decreasing order of magnitude (analogous to PCA). An LV consists of three components: (1) a singular value, (2) a vector of the condition loadings (weights within the left singular value) that represents an underlying contrast among conditions, and (3) a vector of the element loadings (weights within the right singular value) that represents the optimal spatiotemporal distribution (i.e., Sources × Timescale/Frequency) for the given contrast among conditions.

Each LV was statistically evaluated two ways. First, we assessed the significance of the condition contrast represented by a given LV (i.e., condition loading) by determining how different the contrast was from chance. To do this, we computed 500 permutation tests in which conditions were randomly assigned within subjects. A measure of significance was calculated by estimating the proportion of times the permuted singular value was higher than the observed singular value.

Second, to assess the stability of the corresponding spatiotemporal distribution across subjects (i.e., element loading), we resampled subjects within conditions (500 bootstrap samples). The bootstrap ratio provided a measure of stability, which was calculated by taking the ratio of the element loading and the standard error of the generated bootstrap distribution. The bootstrap ratio is approximately equivalent to a z score, whereby an absolute bootstrap ratio greater than 3 corresponds roughly to a 95% confidence interval. For a given LV, brain elements with positive bootstrap ratios supported the depicted contrast among conditions (e.g., A > B > C), whereas brain elements with negative bootstrap ratio supported the inverse of the contrast among conditions (e.g., A < B < C).

RESULTS

Vividness Ratings

As seen in Table 1, PE recordings were associated with higher ratings than GS recordings, confirming the effectiveness of the PE stimuli for evoking richer multimodal episodic recollection. This was supported by a repeated-measures ANOVA with two within-subject factors of Remembering Condition (PE, GS) and Rating Type (thoughts/emotion, visual imagery, episodic fluency, overall vividness), which yielded a significant main effect of Condition, $F(1, 7) = 207$, $p < .001$, $\eta_p^2 = 0.97$.

MEG Data

From the MEG data, we extracted four unique metrics: MSE, local entropy, distributed entropy, and spectral power. Figure 2 depicts the grand mean (collapsed across subjects and sources) for each metric across timescale/frequency, illustrating the intrinsic characteristics of the brain signal related to the rate at which information is

Table 1. Subjective Ratings for PE and GS Memory Conditions

	Thoughts/Emotions	*Visual Imagery*	*Episodic Fluency*	*Overall Vividness*
PE	7.6 (1.0)	7.8 (1.0)	7.8 (.9)	7.8 (.9)
GS	2.4 (1.8)	2.6 (1.6)	1.7 (1.5)	2.3 (1.5)

Ratings were made on four 10-point scales, where the maximum vividness rating was 10. Parentheses indicate standard deviations.

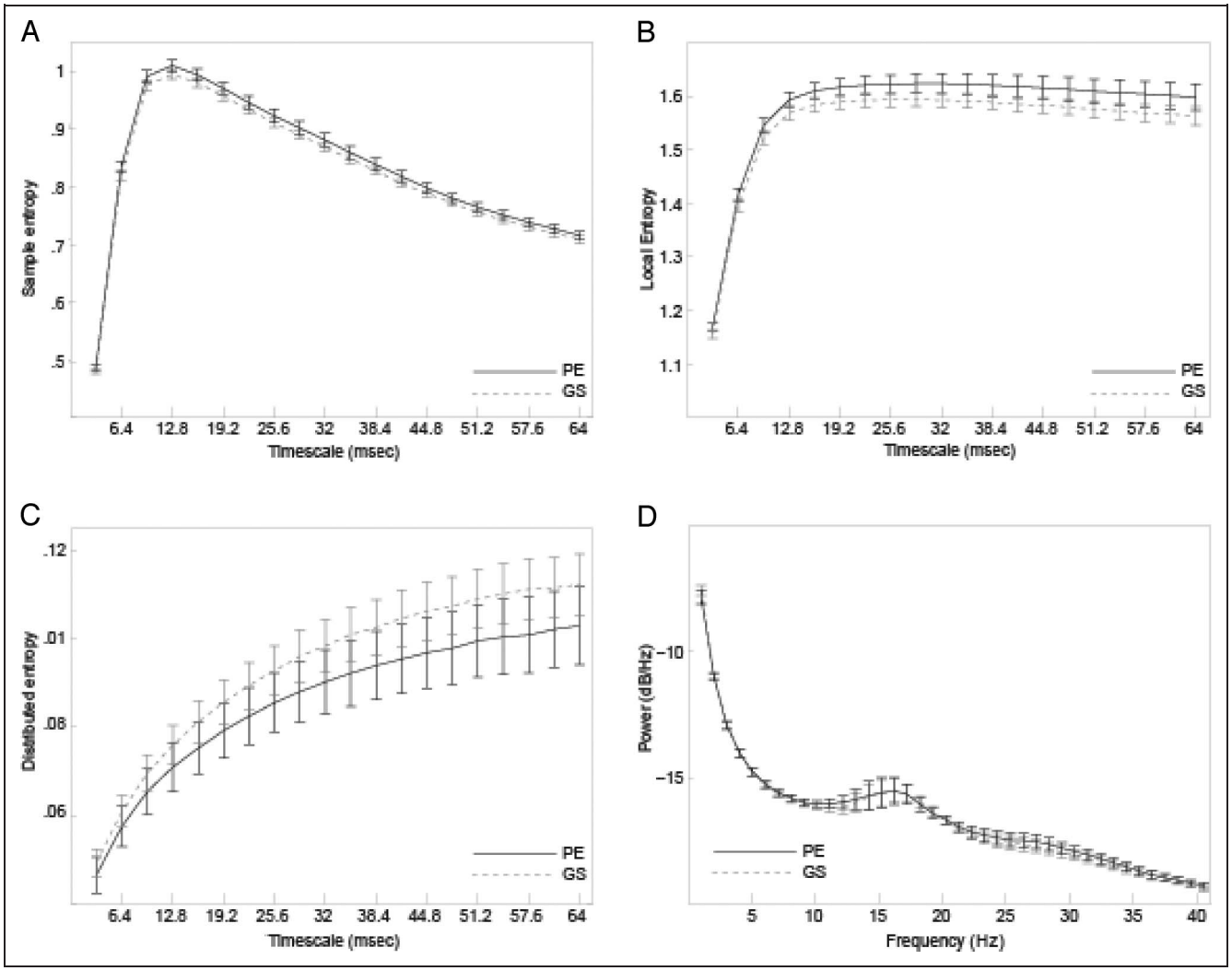

Figure 2. Grand mean response collapsed across all brain sources for (A) MSE, (B) local entropy, (C) distributed entropy, and (D) spectral power. Timescales 1–20 were converted into milliseconds by dividing the timescale by the sampling rate (312.5 Hz).

generated, received, and processed by the ensembles of coupled neural systems. Sample entropy peaked at timescale 12.8 msec and then gradually declined, indicating the peak rate at which information is generated and processed by all sources (Vakorin & McIntosh, 2012). Local entropy rapidly increased to peak at timescale 19.2 msec and then plateaued, indicating that information processed locally across various timescales (Vakorin, Mišić, et al., 2011). Distributed entropy was greater at coarser timescales than finer timescales, suggesting greater information processing between two sources at coarse timescales (Vakorin, Mišić, et al., 2011). Frequency power distribution displays the typical 1/*f* distribution with a peak in the alpha frequency band that is seen for EEG and MEG data and reflects the composition of neural oscillators contributing to the neural signal.

Unlike evoked potentials in which the peak component reflects meaningful stimulus processing stages, the peak response of entropy and spectral power measures reflects the underlying intrinsic characteristics of the signal; therefore, it is possible for the condition differences to be expressed at various points along the distribution.

The condition differences between PE and GS recordings revealed by the PLS analyses are depicted in Table 2 and Figure 3. Table 2 presents the specific contrast among conditions. As seen in Table 2, there were no changes in any of the metrics across the four 6-sec time windows of the PE or GS recordings. Figure 3 illustrates the corresponding spatiotemporal distribution of brain sources and timescales that reliably (i.e., threshold set at the 95th percentile) expressed the condition contrast.

MSE

PLS analysis revealed one significant LV ($p < .001$; Table 2). Only positive bootstrap ratios were reliable (Figure 3A), indicating greater MSE for the PE condition than the GS condition. The spatiotemporal distribution of this condition effect was stable across multiple timescales in the left

Table 2. PLS Results Indicating the Specific Contrast between PE and GS for MSE, Local Entropy, Distributed Entropy, and Spectral Power

	GS		*PE*	
	Mean	*95% CI*	*Mean*	*95% CI*
MSE	−0.25		0.25	
1	−0.29	[−0.51, −0.17]	0.10	[−0.04, 0.38]
2	−0.36	[−1.16, −0.16]	0.30	[0.08, 0.75]
3	−0.37	[−0.88, −0.21]	0.18	[0.09, 0.59]
4	0.02	[−0.15, 0.27]	0.42	[0.25, 0.64]
Local entropy	−0.61		0.61	
1	−0.82	[−1.26, −0.53]	0.30	[−0.08, 0.85]
2	−0.49	[−1.84, 0.14]	0.97	[0.32, 1.68]
3	−0.80	[−1.52, −0.49]	0.44	[0.14, 1.22]
4	−0.35	[−0.65, 0.15]	0.75	[0.31, 1.23]
Distributed entropy	−0.16		0.16	
1	−0.15	[−0.29, 0.01]	0.17	[0.07, 0.31]
2	−0.08	[−0.52, 0.08]	0.14	[−0.03, 0.46]
3	−0.25	[−0.63, −0.08]	0.15	[0.07, 0.38]
4	−0.16	[0.00, 0.33]	0.18	[0.06, 0.30]
Spectral power	−0.06		0.06	
1	−0.09	[−0.15, −0.06]	0.01	[−0.04, 0.08]
2	−0.09	[−0.25, −0.05]	0.10	[0.07, 0.20]
3	−0.05	[−0.12, −0.04]	0.04	[0.02, 0.13]
4	0.00	[−0.05, 0.04]	0.08	[0.04, 0.14]

The 24-sec epoch during the PE and GS recording was evenly divided into four 6-sec bins, 1–4.

dorsolateral and centrolateral PFC, the left ventrolateral premotor cortex, right anterior insula, and right claustrum.

Local Entropy

PLS analysis revealed one significant LV ($p < .001$; Table 2). Only positive bootstrap ratios were reliable (Figure 3B), indicating greater local entropy for the PE condition compared with the GS condition. This condition effect was most stable at timescales greater than 16 msec and was primarily expressed by brain regions of right hemisphere, including primary auditory cortex, anterior insula, claustrum, angular gyrus, and ventrolateral premotor cortex. Only the medial and ventrolateral premotor cortex of the left hemisphere revealed the condition effect.

Distributed Entropy

PLS analysis revealed one significant LV ($p < .01$; Table 2). Only negative bootstrap ratios were reliable (Figure 2C), corresponding to greater distributed entropy for the GS condition compared with the PE condition. This condition effect was most stable at timescales greater than 16 msec for the retrosplenial cingulate cortex, left thalamus, and right angular gyrus.

Spectral Power

PLS analysis revealed one significant LV ($p < .001$; Table 2). Both positive and negative bootstrap ratios were reliable (Figure 2D), indicating an interaction between the condition and the particular spatiotemporal distribution (Source × Frequency). For example, the condition effect in the left centrolateral PFC depended on the carrier frequencies. This was also observed for the bilateral ventrolateral premotor and right anterior insula.

DISCUSSION

This study used information theoretic measures of entropy to quantify changes in the complexity of the brain's response while participants listen to audio recordings of past PE and GS events. We manipulated the richness of the associated mnemonic content (autobiographical episodic vs. semantic) while keeping constant the superficial elements of the conditions (i.e., listening to information recorded in one's own voice). PE recordings evoked richer subjective mnemonic experiences and more complex brain responses than GS recordings. Moreover, the relative contribution of local versus distributed entropy varied across conditions; PE recordings elicited relatively more local entropy than GS recordings, whereas GS recordings elicited relatively more distributed entropy than PE recordings. This trade-off between local and distributed information processing may provide a potential mechanism that allows the same network of brain regions to represent both event-specific and general information.

Across the entire length of the trial, the rich cognitive experience of recalling a past personal event produced a relatively more complex brain response than recalling more GS information. Consistent with previous functional neuroimaging studies of autobiographical memory (Cabeza & St Jacques, 2007; Svoboda et al., 2006; Maguire, 2001), condition differences between autobiographical and semantic memory were expressed in the left prefrontal regions that are involved in higher mnemonic retrieval operations. However, we did not expect the spatial contrast to perfectly match across measures of dynamic information processing and those of average brain activation. Indeed, our analysis indicated greater complexity for autobiographic versus semantic memory in the right insula—a region that is typically not activated in fMRI studies of autobiographical memory (Svoboda et al., 2006; but it was observed in a study using this recordings paradigm, Svoboda & Levine, 2009). The recruitment of the right insula may reflect greater information processing related to the interoceptive states evoked when recollecting

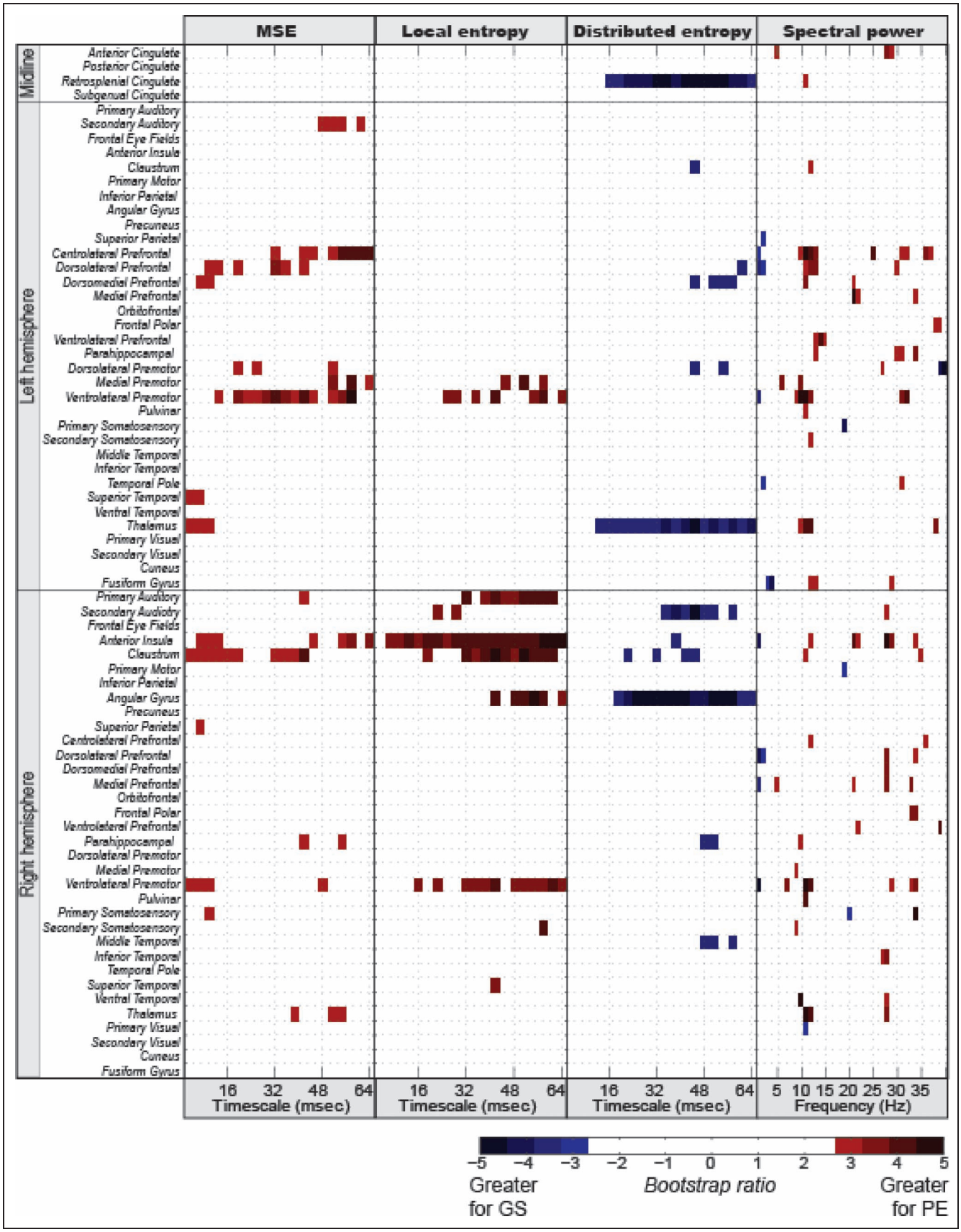

Figure 3. PLS results depicting the spatiotemporal distribution of brain sources and timescales that reliably (i.e., threshold set at the 95th percentile) expressed the condition contrast for MSE, local entropy, distributed entropy, and spectral power. Timescales 1–20 were converted into milliseconds by dividing the timescale by the sampling rate (312.5 Hz).

autobiographical events (Singer, Critchley, & Preuschoff, 2009).

Consistent with previous results (Heisz et al., 2012; Misic et al., 2010), brain signal complexity increased with the amount of meaningful cognitive information available for stimulus processing. This observation is also consistent with the theoretical framework of complexity matching, which asserts that the amount of information available to the system is related to the match between the complexity of the stimulus and the complexity of the corresponding brain response (Tononi, Sporns, & Edelman, 1996). The amount of information retrieved may also depend on the extent to which the retrieval cue reinstates the context associated with the event at the time of encoding. The PE recordings were created proximally to the event and thus were highly potent retrieval cues; that is, they evoked a rich, multimodal retrieval experience optimized for correspondence to the sensory information present at the time of encoding.

The observed change in brain signal complexity may reflect transitions or bifurcations between microstates of a network; different aspects of the memory are stored in unique microstates, and as the network explores those microstates the information becomes available to the system. The representation of episodic autobiographical memory, with the additional details regarding the self in a particular past time and place plus associated emotional and perceptual information (Table 1), may activate a network with a greater number of microstates than GS memory and thus produce a more complex brain response. Critically, this stimulus-evoked complexity differs from general intrinsic complexity. General intrinsic complexity refers to the information processing capacity of the entire brain system that changes across development (Lippe et al., 2009; McIntosh et al., 2008) and as a consequence of brain injury (Raja, Kovačević, McIntosh, & Levine, 2012) and neurodegenerative disease (Park et al., 2007), for example. In contrast, stimulus-evoked complexity reflects the amount of cognitive information that is available for a particular event or task and thus can vary transiently within brain systems depending on the current cognitive operations.

Parsing the total stimulus-evoked complexity into local versus distributed contributions revealed a unique trade-off between local and distributed entropy. Episodic autobiographical memory elicited relatively more local entropy and relatively less distributed entropy than GS memory. Greater information processing by local generators may facilitate the retrieval of the unique details associated with a specific autobiographical event. In contrast, greater distributed information processing across a network of brain regions may enable the representation of redundant or shared information within a network and thus facilitate GS knowledge representation. Interestingly, a common network of brain regions participated in this trade-off showing greater local entropy during the PE recordings and greater distributed entropy during the GS recordings (Figure 3B vs. C). This network of regions included the right anterior insula, right claustrum, right angular gyrus, and right secondary auditory cortex. The recruitment of similar brain regions to support both local and distributed information processing suggests the possibility that these regions may be involved in transiently biasing the way in which information is represented by the system. The right angular gyrus is particularly well positioned for such a role as a multimodal processing region (Seghier, 2012). This region is part of a bottom–up frontoparietal alerting network that is engaged by salient stimuli (Corbetta & Shulman, 2002), such as high-confidence recognition and recollection signals from the medial-temporal lobe (Cabeza, Ciaramelli, Olson, & Moscovitch, 2008; Wagner, Shannon, Kahn, & Buckner, 2005), and thus may be involved in biasing the system toward either episodic or semantic information, depending on the network dynamics. Such a mechanism would allow for both PE and GS information to be derived from a common collection of past experiences (Conway & Pleydell-Pearce, 2000).

There were also several brain regions that showed reliable effects for either distributed entropy or local entropy only. For example, the bilateral ventrolateral premotor areas displayed condition differences in local entropy but not distributed entropy. In contrast, the retrosplenial cingulate and the left thalamus displayed condition differences in distributed entropy but not local entropy. BOLD activation in the retrosplenial cortex and some thalamic nuclei are similar for GS and PE recordings (Svoboda & Levine, 2009), whereas we observed greater distributed entropy for GS than PE recording. The retrosplenial cortex is a hub region (Vann, Aggleton, & Maguire, 2009) where more distributed connectivity might be expected. The differences between the current study that used complexity measures and previous reports that used mean-based measures suggest the possibility that complexity measures are sensitive to unique aspects of the data that traditional mean-based measures may not detect; however, future research that concurrently measures brain signal complexity and BOLD activity and uses the same statistical platform for data analysis is needed to provide direct evidence to support this claim.

Although previous work has demonstrated that the same quantitative framework is capable of identifying opposite patterns across the two measures (McIntosh et al., 2013; Vakorin, Lippé, et al., 2011), differences in brain signal complexity between the PE and GS recordings were expressed in a consistent manner across each information theoretic metric. For example, all brain regions and timescales that expressed reliable condition differences in local entropy displayed greater local entropy for PE than GS recordings. In contrast, although certain frequencies expressed greater power for the PE over GS recordings, the effects of spectral power varied across brain regions and frequencies, suggesting that differences in complexity between PE and GS conditions did not result from differences in the oscillatory activity of a particular

carrier frequency or by global differences in broadband activity. This is consistent with previous reports that have used simulations to demonstrate that the effects of signal complexity do not merely reflect changes in broadband spectral power (McIntosh et al., 2008). Specifically, previous studies have demonstrated that modifying the original signal by either increasing power at lower frequencies and decreasing power at higher frequencies, or through phase randomization, do not affect total spectral power but does affect the complexity of the signal (McIntosh et al., 2008). Thus, it is unlikely that broadband signals are the sole cause of the observed entropy patterns; instead, the observed entropy patterns may be driven by narrowband power changes, phase change, or nonlinear modulations. Future work is needed to further examine the underlying neural sources that produced the observed differences in entropy.

Linear measures of connectivity based on spectral coherence provide complementary information about the neural processes that underlie memory retrieval. Using the same data set, Fuentemilla, Barnes, Duzel, & Levine (2013) observed greater theta-phase synchronization of the left hippocampus with the precuneus and medial PFC for PE over GS recordings. Theta-phase synchronization may provide a potential mechanism by which information is transferred between the hippocampus and neocortex; in contrast, entropy may index the integration and processing of that information within distributed networks. More work is needed to understand the relationship between these two complementary measures of connectivity.

In conclusion, PE memories elicited a richer cognitive experience and produced a more complex brain response. This further supports the claim that brain signal complexity provides a window onto the amount of cognitive information that is available for a task. We also observed a trade-off in the relative amounts of local versus distributed entropy within the same network of regions for episodic versus semantic retrieval. This points to a potential mechanism by which the same network of regions are recruited for the representation of both event-specific and general information, such that a relative increase in local entropy promotes event-specific details whereas a relative increase in distributed entropy promotes more GS representations.

Acknowledgments

Sabitha Kanagasabai and Tim Bardouille are thanked for technical assistance. This research was supported by a James S. McDonnell Foundation grant awarded to A. R. M. and by the Canadian Institutes of Health Research Grant MGP-62963 and the National Institute of Child Health and Human Development, National Institutes of Health Grant HD42385-01 to B. L.

Reprint requests should be sent to Jennifer J. Heisz, Department of Kinesiology, McMaster University, 1280 Main Street West, Hamilton, Ontario, Canada, L8S 4K1, or via e-mail: heiszjj@mcmaster.ca, Website: www.jenniferheisz.ca.

REFERENCES

Bezgin, G., Vakorin, V. A., van Opstal, A. J., McIntosh, A. R., & Bakker, R. (2012). Hundreds of brain maps in one atlas: Registering coordinate-independent primate neuro-anatomical data to a standard brain. *Neuroimage, 62,* 67–76.

Breakspear, M. (2002). Nonlinear phase desynchronization in human electroencephalographic data. *Human Brain Mapping, 15,* 175–198.

Bressler, S. L., & McIntosh, A. R. (2007). The role of neural context in large-scale neurocognitive network operations. In V. K. Jirsa & A. R. McIntosh (Eds.), *Handbook of brain connectivity* (pp. 403–420). Heidelberg, Germany: Springer.

Burianova, H., & Grady, C. L. (2007). Common and unique neural activations in autobiographical, episodic, and semantic retrieval. *Journal of Cognitive Neuroscience, 19,* 1520–1534.

Burianova, H., McIntosh, A. R., & Grady, C. L. (2010). A common functional brain network for autobiographical, episodic, and semantic memory retrieval. *Neuroimage, 49,* 865–874.

Cabeza, R., Ciaramelli, E., Olson, I. R., & Moscovitch, M. (2008). The parietal cortex and episodic memory: An attentional account. *Nature Reviews Neuroscience, 9,* 613–625.

Cabeza, R., & St Jacques, P. (2007). Functional neuroimaging of autobiographical memory. *Trends in Cognitive Sciences, 11,* 219–227.

Conway, M. A., & Pleydell-Pearce, C. W. (2000). The construction of autobiographical memories in the self-memory system. *Psychological Review, 107,* 261.

Corbetta, M., & Shulman, G. L. (2002). Control of goal-directed and stimulus-driven attention in the brain. *Nature Reviews Neuroscience, 3,* 201–215.

Costa, M., Goldberger, A. L., & Peng, C. K. (2005). Multiscale entropy analysis of biological signals. *Physical Review E: Statistical, Nonlinear, and Soft Matter Physics, 71,* 021906.

Deco, G., Jirsa, V. K., & McIntosh, A. R. (2011). Emerging concepts for the dynamical organization of resting-state activity in the brain. *Nature Reviews Neuroscience, 12,* 43–56.

Deco, G., Jirsa, V., McIntosh, A., Sporns, O., & Kötter, R. (2009). Key role of coupling, delay, and noise in resting brain fluctuations. *Proceedings of the National Academy of Sciences, 106,* 10302–10307.

Engel, A. K., Fries, P., & Singer, W. (2001). Dynamic predictions: Oscillations and synchrony in top-down processing. *Nature Reviews Neuroscience, 2,* 704–716.

Freeman, W. J., & Rogers, L. J. (2002). Fine temporal resolution of analytic phase reveals episodic synchronization by state transitions in gamma EEGs. *Journal of Neurophysiology, 87,* 937–945.

Friston, K. J. (2000). The labile brain. I. Neuronal transients and nonlinear coupling. *Philosophical Transactions of the Royal Society, Series B, Biological Sciences, 355,* 215.

Fuentemilla, L., Barnes, G. R., Duzel, E., & Levine, B. (2013). Theta oscillations orchestrate medial temporal lobe and neocortex in remembering autobiographical memories. *Neuroimage*. doi:10.1016/j.neuroimage.2013.08.029.

Gatlin, L. L. (1972). *Information theory and the living system* (Vol. 1). New York: Columbia University Press.

Ghosh, A., Rho, Y., McIntosh, A. R., Kotter, R., & Jirsa, V. K. (2008). Cortical network dynamics with time delays reveals functional connectivity in the resting brain. *Cognitive Neurodynamics, 2,* 115–120.

Gilboa, A. (2004). Autobiographical and episodic memory-one and the same?: Evidence from prefrontal activation in neuroimaging studies. *Neuropsychologia, 42,* 1336–1349.

Heisz, J. J., & McIntosh, A. R. (2013). Applications of EEG neuroimaging data: Event-related potentials, spectral power, and multiscale entropy. *Journal of Visualized Experiments: JoVE, 76,* doi:10.3791/50131.

Heisz, J. J., Shedden, J. M., & McIntosh, A. R. (2012). Relating brain signal variability to knowledge representation. *Neuroimage, 63,* 1384–1392.

Holmes, C. J., Hoge, R., Collins, L., Woods, R., Toga, A. W., & Evans, A. C. (1998). Enhancement of MR images using registration for signal averaging. *Journal of Computer Assisted Tomography, 22,* 324–333.

Honey, C. J., Kotter, R., Breakspear, M., & Sporns, O. (2007). Network structure of cerebral cortex shapes functional connectivity on multiple time scales. *Proceedings of the National Academy of Sciences, U.S.A., 104,* 10240–10245.

Jirsa, V. K., & McIntosh, A. R. (2007). *Handbook of brain connectivity* (Vol. 1). Berlin: Springer.

Kotter, R., & Wanke, E. (2005). Mapping brains without coordinates. *Philosophical Transactions of the Royal Society of London, Series B, Biological Sciences, 360,* 751–766.

Kraskov, A., Stögbauer, H., & Grassberger, P. (2004). Estimating mutual information. *Physical Review E, 69,* 066138.

Lake, D. E., Richman, J. S., Griffin, M. P., & Moorman, J. R. (2002). Sample entropy analysis of neonatal heart rate variability. *American Journal of Physiology-Regulatory, Integrative and Comparative Physiology, 283,* R789–R797.

Levine, B., Turner, G. R., Tisserand, D., Hevenor, S. J., Graham, S. J., & McIntosh, A. R. (2004). The functional neuroanatomy of episodic and semantic autobiographical remembering: A prospective functional MRI study. *Journal of Cognitive Neuroscience, 16,* 1633–1646.

Lippe, S., Kovacevic, N., & McIntosh, A. R. (2009). Differential maturation of brain signal complexity in the human auditory and visual system. *Frontiers in Human Neuroscience, 3,* 48.

Lobaugh, N. J., West, R., & McIntosh, A. R. (2001). Spatiotemporal analysis of experimental differences in event-related potential data with partial least squares. *Psychophysiology, 38,* 517–530.

Maguire, E. A. (2001). Neuroimaging studies of autobiographical event memory. *Philosophical Transactions of the Royal Society of London, Series B, Biological Sciences, 356,* 1441–1451.

McClelland, J. L., & Rumelhart, D. E. (1985). Distributed memory and the representation of general and specific information. *Journal of Experimental Psychology: General, 114,* 159.

McDermott, K. B., Szpunar, K. K., & Christ, S. E. (2009). Laboratory-based and autobiographical retrieval tasks differ substantially in their neural substrates. *Neuropsychologia, 47,* 2290–2298.

McIntosh, A. R., Kovacevic, N., & Itier, R. J. (2008). Increased brain signal variability accompanies lower behavioral variability in development. *PLoS Computational Biology, 4,* e1000106.

McIntosh, A., Vakorin, V., Kovacevic, N., Wang, H., Diaconescu, A., & Protzner, A. (2013). Spatiotemporal dependency of age-related changes in brain signal variability. *Cerebral Cortex*. doi:10.1093/cercor/bht030.

Misic, B., Mills, T., Taylor, M. J., & McIntosh, A. R. (2010). Brain noise is task dependent and region specific. *Journal of Neurophysiology, 104,* 2667–2676.

Mišić, B., Vakorin, V. A., Paus, T., & McIntosh, A. R. (2011). Functional embedding predicts the variability of neural activity. *Frontiers in Systems Neuroscience, 5,* 90.

Nunez, P. L., & Srinivasan, R. (2005). *Electric fields of the brain: The neurophysics of EEG*. New York: Oxford University Press.

Park, J., Kim, S., Kim, C., Cichocki, A., & Kim, K. (2007). Multiscale entropy analysis of EEG from patients under different pathological conditions. *Fractals-Complex Geometry Patterns and Scaling in Nature and Society, 15,* 399–404.

Prichard, D., & Theiler, J. (1995). Generalized redundancies for time series analysis. *Physica D: Nonlinear Phenomena, 84,* 476–493.

Raja, B. A., Kovačević, N., McIntosh, A., & Levine, B. (2012). Brain signal variability relates to stability of behavior after recovery from diffuse brain injury. *Neuroimage, 60,* 1528.

Rajah, M. N., & McIntosh, A. R. (2005). Overlap in the functional neural systems involved in semantic and episodic memory retrieval. *Journal of Cognitive Neuroscience, 17,* 470–482.

Renoult, L., Davidson, P. S. R., Palombo, D. J., Moscovitch, M., & Levine, B. (2012). Personal semantics: At the crossroads of semantic and episodic memory. *Trends in Cognitive Sciences, 16,* 550–558.

Richman, J. S., & Moorman, J. R. (2000). Physiological time-series analysis using approximate entropy and sample entropy. *American Journal of Physiology. Heart and Circulatory Physiology, 278,* H2039–H2049.

Robinson, S., & Vrba, J. (1999). Functional neuroimaging by synthetic aperture magnetometry (SAM). *Recent Advances in Biomagnetism, 1999,* 302–305.

Sakurai, Y. (1999). How do cell assemblies encode information in the brain? *Neuroscience & Biobehavioral Reviews, 23,* 785–796.

Seghier, M. L. (2012). The angular gyrus: Multiple functions and multiple subdivisions. *The Neuroscientist, 19,* 43–61.

Shannon, C. (1948). A mathematical theory of communication. *Bell System Technical Journal, 27,* 379–423.

Singer, T., Critchley, H. D., & Preuschoff, K. (2009). A common role of insula in feelings, empathy and uncertainty. *Trends in Cognitive Sciences, 13,* 334–340.

Sporns, O., Chialvo, D. R., Kaiser, M., & Hilgetag, C. C. (2004). Organization, development and function of complex brain networks. *Trends in Cognitive Sciences, 8,* 418–425.

Stam, C. J. (2005). Nonlinear dynamical analysis of EEG and MEG: Review of an emerging field. *Clinical Neurophysiology, 116,* 2266–2301.

Steinstraeter, O., Teismann, I. K., Wollbrink, A., Suntrup, S., Stoeckigt, K., Dziewas, R., et al. (2009). Local sphere-based co-registration for SAM group analysis in subjects without individual MRI. *Experimental Brain Research, 193,* 387–396.

Svoboda, E., & Levine, B. (2009). The effects of rehearsal on the functional neuroanatomy of episodic autobiographical and semantic remembering: A functional magnetic resonance imaging study. *The Journal of Neuroscience, 29,* 3073–3082.

Svoboda, E., McKinnon, M. C., & Levine, B. (2006). The functional neuroanatomy of autobiographical memory: A meta-analysis. *Neuropsychologia, 44,* 2189–2208.

Thompson, C. P. (1982). Memory for unique personal events: The roommate study. *Memory & Cognition, 10,* 324–332.

Tononi, G., Edelman, G. M., & Sporns, O. (1998). Complexity and coherency: Integrating information in the brain. *Trends in Cognitive Sciences, 2,* 474–484.

Tononi, G., Sporns, O., & Edelman, G. M. (1996). A complexity measure for selective matching of signals by the brain. *Proceedings of the National Academy of Sciences, U.S.A., 93,* 3422–3427.

Tulving, E. (2002). Episodic memory: From mind to brain. *Annual Review of Psychology, 53,* 1–25.

Vakorin, V. A., Lippé, S., & McIntosh, A. R. (2011). Variability of brain signals processed locally transforms into higher connectivity with brain development. *The Journal of Neuroscience, 31,* 6405–6413.

Vakorin, V. A., & McIntosh, A. R. (2012). Mapping the multi-scale information content of complex brain signals. In M. I. Rabinovič, K. J. Friston, & P. Varona (Eds.), *Principles of brain dynamics: Global state interactions* (pp. 183–208). Cambridge, MA: MIT Press.

Vakorin, V. A., Mišić, B., Krakovska, O., & McIntosh, A. R. (2011). Empirical and theoretical aspects of generation and transfer of information in a neuromagnetic source network. *Frontiers in Systems Neuroscience, 5,* 96.

Van Veen, B. D., Van Drongelen, W., Yuchtman, M., & Suzuki, A. (1997). Localization of brain electrical activity via linearly constrained minimum variance spatial filtering. *Biomedical Engineering, IEEE Transactions on, 44,* 867–880.

Vann, S. D., Aggleton, J. P., & Maguire, E. A. (2009). What does the retrosplenial cortex do? *Nature Reviews Neuroscience, 10,* 792–802.

Varela, F., Lachaux, J. P., Rodriguez, E., & Martinerie, J. (2001). The brainweb: Phase synchronization and large-scale integration. *Nature Reviews Neuroscience, 2,* 229–239.

Wagner, A. D., Shannon, B. J., Kahn, I., & Buckner, R. L. (2005). Parietal lobe contributions to episodic memory retrieval. *Trends in Cognitive Sciences, 9,* 445–453.

Welch, P. (1967). The use of fast Fourier transform for the estimation of power spectra: A method based on time averaging over short, modified periodograms. *Audio and Electroacoustics, IEEE Transactions on, 15,* 70–73.

Wheeler, M. A., Stuss, D. T., & Tulving, E. (1997). Toward a theory of episodic memory: The frontal lobes and autonoetic consciousness. *Psychological Bulletin, 121,* 331.